Design and Simulation of a Slice-Rail with Multi Projectile and Coaxial Railguns using 2D-FEM

S. Mozafari[1]; M. Sajjad Bayati[2,*]

1- Department of Electrical Engineering Razi University, Kermanshah, Iran
2- Department of Electrical Engineering Razi University, Kermanshah, Iran, Email: s.bayati@razi.ac.ir
*Corresponding author
Received: 2019-12-11
Revised: 2020-06-22, 2020-08-27, 2020-09-14
Accepted: 2020-10-08

Abstract Railguns has been researched considerably in recent years. Most of these researches is done to improve the main features of railgun, such as, increment of gradient of inductance L', more uniform current density distributions, and launch synchronously multi projectiles per shot. In this paper, first the slice-rail railgun is presented and simulated by ANSYS software. Then, double and quad slice-rail with one axial is presented for multi-projectile shooting. Finally, the complete case of this slice-rail structure is studied as coaxial railgun. The geometry of slice-rail railgun has inner rail radii (R_i) and width (R_1), outer rail radii (R_o) and width (R_2) and the total angle of curved rails (θ). Current density distribution, Magnetic flux density and inductance gradient are computed for slice and coaxial railgun. Magnetic field at the outside of the muzzle for slice railgun with θ =90˚ is computed and compared with rectangular railgun meanwhile L' equals to 0.45 μH/m for both railguns.

Keywords: Coaxial Railgun, current distribution, finite element method, inductance gradient, multi-projectile.

1. Introduction

Railgun accelerates an armature to very high velocities by electric energy. There are many feasible industrial and military applications that need such a structure [1, 2]. In its simplest form, railgun is made of two parallel long conductors, rails and a conductor between them, armature that is very small in comparison with rails, because it is picked to be accelerated and launched. The exerted magnetic force on the armature is Lorentz force. The total force can be calculated by the integration of the **J**×**B** over the armature volume in which, **B** and **J** are the magnetic flux density and current density, respectively [3, 4]. Magnetic force can be computed by using gradient of magnetic energy. Magnetic energy and force can be found to be,

$$W_m = \frac{1}{2} L I^2 \tag{1}$$

$$F = \nabla W_m = \frac{1}{2} L' I^2 \tag{2}$$

I is applied current and L' is inductance gradient which depends on the geometrical shape and the physical arrangement of the rails. Numerical methods such as finite element, boundary element and method of moment are reported for electromagnetic simulation in [5- 9]. Current distribution and inductance gradient in a railgun have a special role which is affected by shape of rails [3, 4], [10-13]. Multi-projectile railguns are novel electromagnetic launchers can be shooting two or more projectiles per shot [14, 15]. Coaxial railgun is reported in [16, 17]. Inductance gradient formula for a coaxial railgun can be written as [16],

$$L' = \frac{\mu_0}{2\pi} ln\left(\frac{b}{a}\right) \tag{3}$$

where b and a are outer and inner radius of the coaxial railgun, respectively.

In this paper, first the slice-rail railgun is presented and simulated by ANSYS software. Then, double and quad slice-rail with one axial is presented for multi-projectile shooting. Finally, the complete case of this slice-rail structure is studied as coaxial railgun. By using unequal circular rails we actuate to coaxial multi-projectile structures and even complete coaxial railgun that has none sharp edges and corners. By completing the curved rails in a cylindrical structure, the magnetic field distributions have been changed to circles inbound in the bore of launcher. Current density distribution, Magnetic flux density and inductance gradient are computed for slice and coaxial railgun. The aims of this paper are reduced the magnetic field out of the railgun's bore and a uniform current distribution on the cross section of the rail is obtained.

2. Slice-Rail railgun

Railgun with parallel rails is a common structure. Rectangular, concave, convex and circular parallel rails are considered and simulated extensively [10-13]. The magnetic field lines around parallel rails for different cross-sections, are shown in Fig. 1.

The density of magnetic field line in bore or between the parallel rails, is more intensive than outside of bore. The magnetic field outside of the bore influences on nearby electronic equipment which is undesirable.

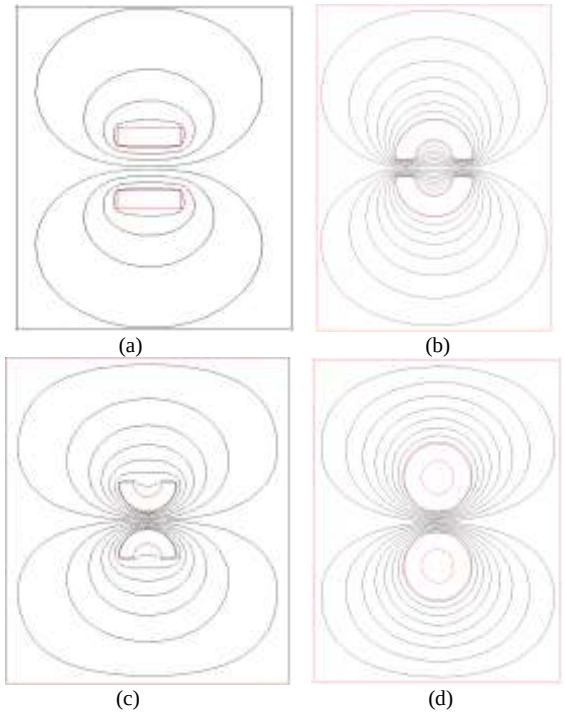

Fig. 1. The magnetic flux lines. (a) two parallel rectangular rails, (b) two parallel concave curved rails, (c) two parallel convex curved rails, (d) two parallel circular ring rails.

2.1. Introduction and geometry of the slice-rail

To study unequal rail structures, there are many feasible designs that can be considered, such as a parallel rectangular railgun in which height or width of rails are unequal or generally railguns with different shapes and geometries for each rail. We considered a concave-convex pair of rails in which convex rail is smaller and both rails are concentric. This slice-rail railgun could be expanded to a multi-projectile railgun by using more pairs that has been studied later, in the next section. The geometry of slice-rail railgun is shown in Fig.2 where R_i, R_o and θ are inner rail radii, outer rail radii, and the total angle of curved rails correspondingly. R_1 determines the widths of inner rail and R_2 does the same for outer rail.

2.2. Magnetic Flux Line, Current Distribution and Inductance Gradient

When both of rails are concave or convex, not only there are no improvement in current density distributions but the gradient inductance of the structure will be decreased. This is because of parallel currents in both edges of a rail that have opposite effects in the barrel. Consequently, this weakens the net magnetic field in the barrel. Thus, in a railgun with a concave-convex pair rails, it is obvious that there is no considerable improvement, such as increment in L' or decrement in density of high current spots. So it sounds that with equal rail structures, our major goals could not be achieved acceptably and unequal structures might be a better option.

The magnetic flux line of the sectional railgun has been shown in Fig.3 for θ =120°, 180°, 240°, and 300°.

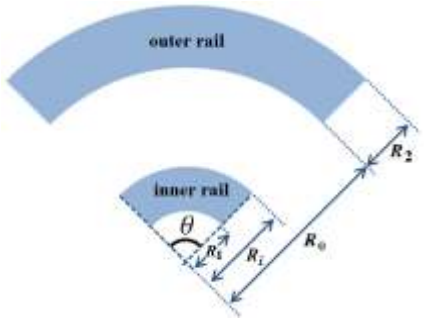

Fig. 2. Cross-Section of the slice-railgun

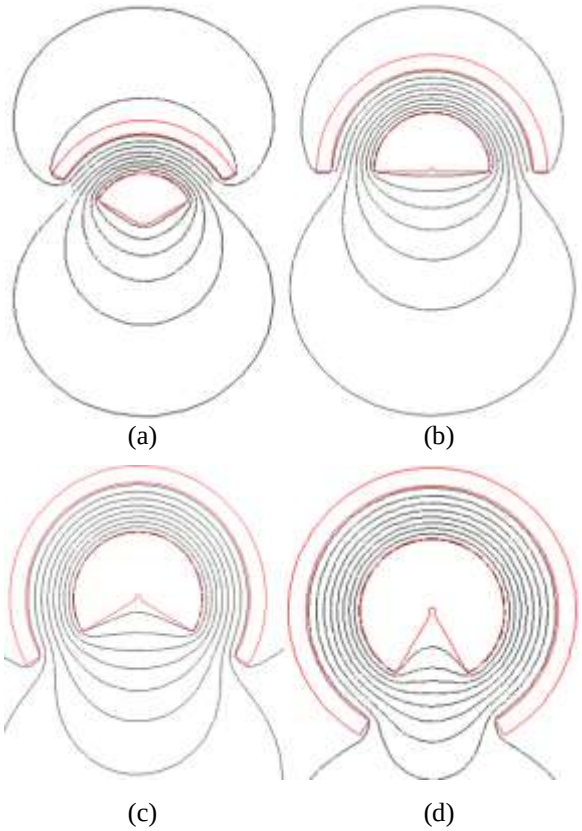

Fig. 3. The magnetic flux line of the slice-railgun for various θ. (a) θ=120º, (b) θ=180º, (c) θ=240º, (d) θ=300º

Likewise, parallel railgun, the magnetic flux lines need some space around rail conductors to develop closed paths. Because of that there is unwanted radiation and strong fields around the structure. Containment is urgent for this structure, because the net force on each rail is repulsive and propels both of them likewise parallel railgun. Furthermore, this imposes major limitations in the case of material selection for the containment, because it should be magnetically transparent thus metal material should be canceled out.

The current density distribution on the rails cross-section for θ =120°, 180° and 240° has been shown in Fig. 4. The rail material is considered to be copper. As it is respected, the high current density spots are located at edges and corners and as it can be seen, the current density distribution for larger θ is more uniform and its maximum value in each rail has been decreased subsequently.

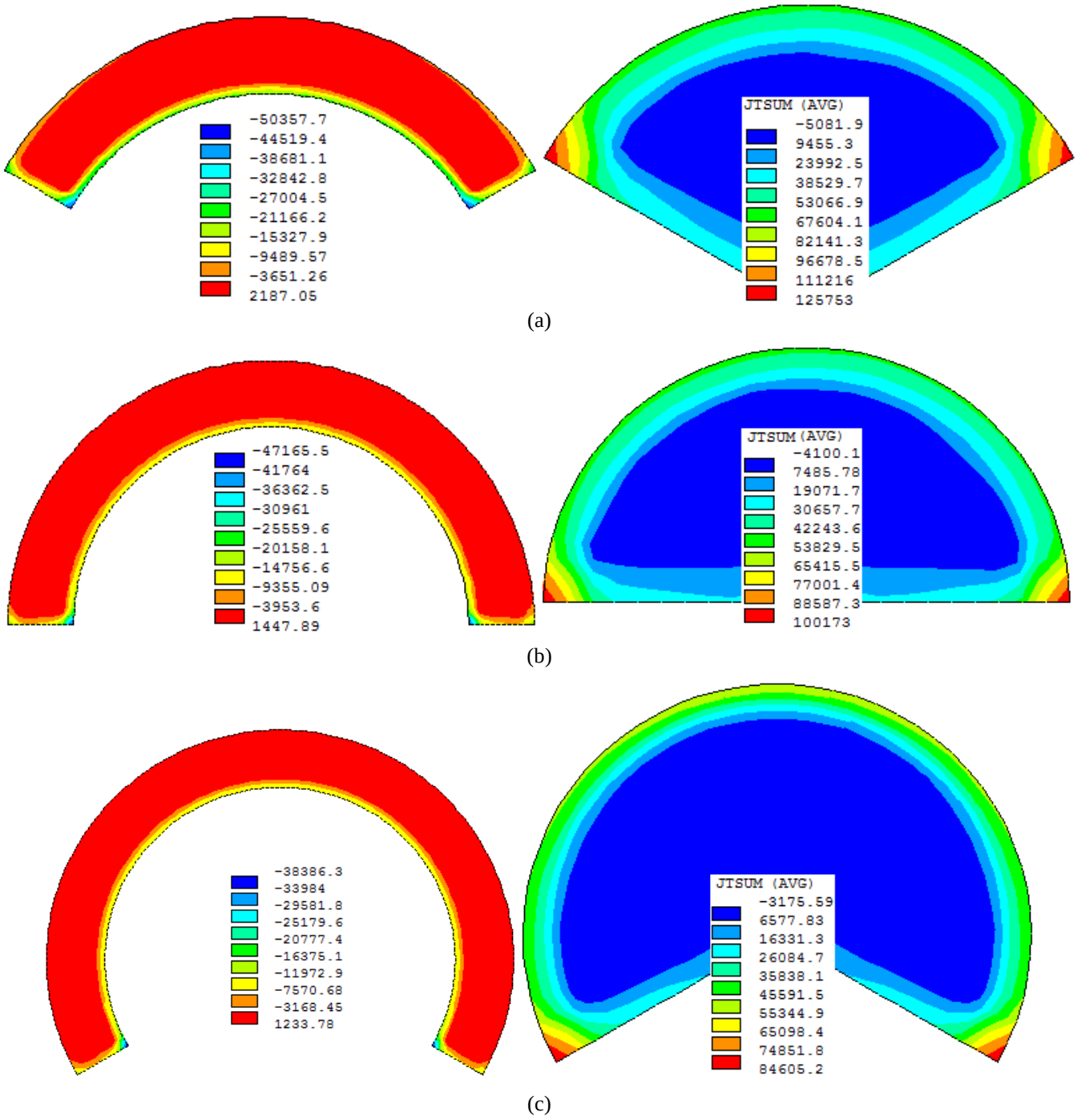

Fig. 4. Current distribution for various θ, R_1=1 mm, R_i=10 mm, R_o=30 mm and R_2=40 mm. (a) θ=120º, (b) θ=180º, (c) θ=240º.

For a railgun with R_i=4 mm and R_o=35 mm, the maximum current density on both rails versus angle θ has been shown in Fig. 5. By increasing the angle θ, the maximum of current density distribution in each rail is decreased. In this case the decrement is more than 10 times in both rails. By increasing the angle of curved rails, the current density distribution becomes more uniform. In the case of θ=360º, which is a complete coaxial structure, the current density distribution is ideal uniform one, leastwise at the surface of each rail.

By increasing the angle θ, there are two parallel currents in the same direction on opposite edges of the outer rail which means a severe decrement in the magnetic field intensity between them. Thus a decreasing gradient inductance L' versus angle θ is reasonable. It is similar to the effects of height increasing in rectangular rail ones. Actually, if a rectangular-rail EML with one overhung rail has been curved then a slice-rail EML will be made. The gradient inductance L' versus angle θ for different ratio of R_o/R_i has been shown in Fig. 6.

2.3. Comparison between rectangular and slice railgun

The magnetic field outside of the bore influences on nearby electronic equipment which is undesirable. To compare the magnetic field performance of the rectangular and slice railgun at the outside of the bore, first both railgun assumed to have same inductance gradient and equals to 0.45 μH/m.

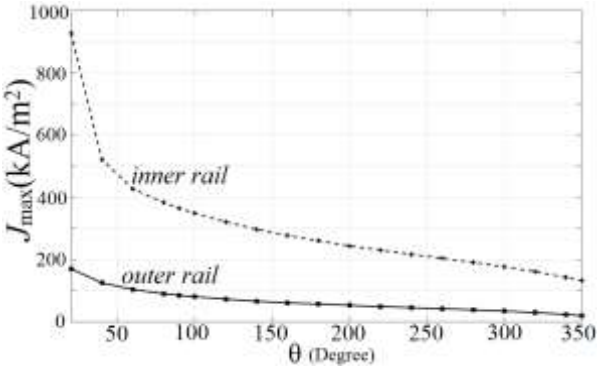

Fig. 5. The maximum of current density in each rail for various θ, R_1=1 mm, R_i=4mm, R_o=35mm and R_2=40mm

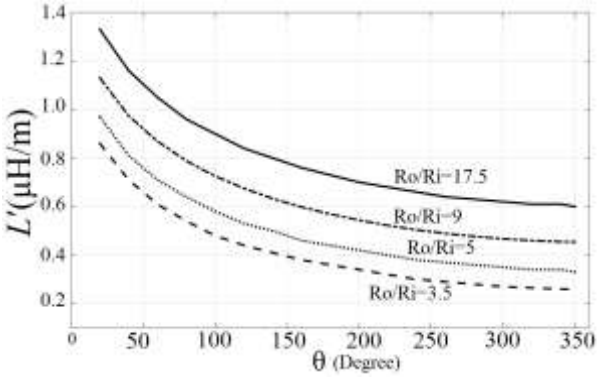

Fig. 6. The gradient inductance L' versus θ for different R_o/R_i.

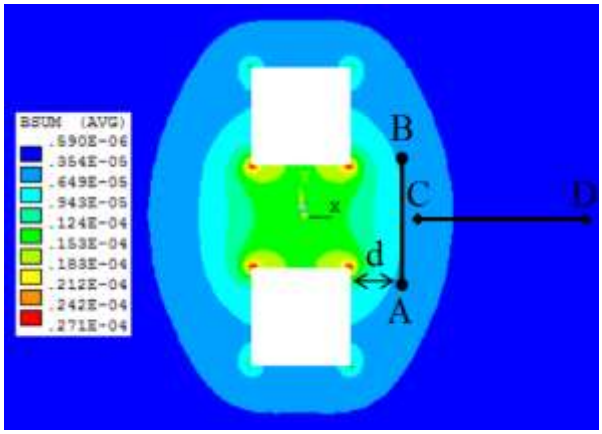

(a)

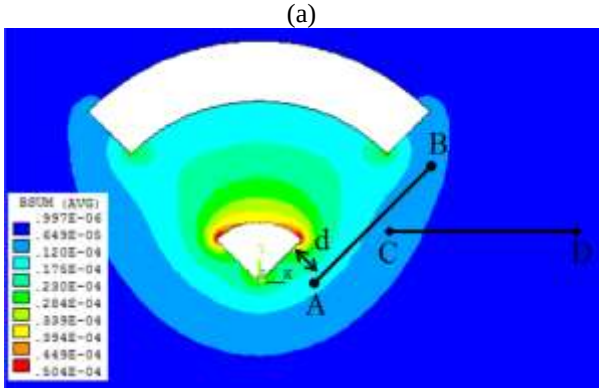

(b)

Fig. 7. Magnetic flux density distribution. (a) rectangular railgun with s=h=w=3 cm, (b) slice railgun with R_i=1 cm, R_o=3 cm, R_1=1 cm and θ=90˚

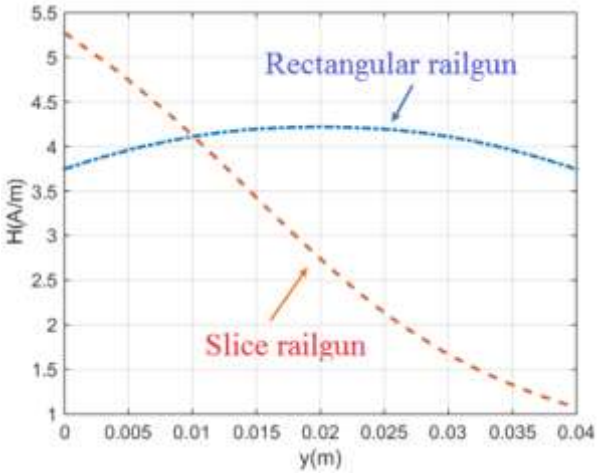

(a)

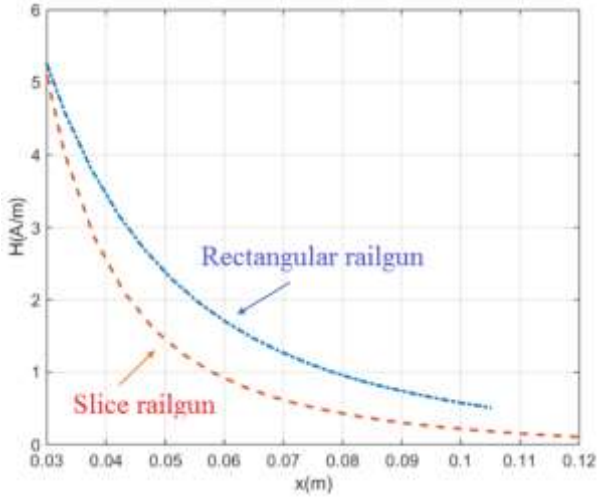

(b)

Fig. 8. Comparison the magnetic field intensity between rectangular railgun (blue dash-dot line) and slice railgun (red dash-line). (a) AB, (b) CD

For L'=0. 45 μH/m, the rectangular railgun has s=h=w= 3 cm, and slice railgun has R_i=1 cm, R_o=3 cm, R_1=1 cm and θ=90˚. Magnetic field is computed for both railgun and shown in Fig. 7.

It is difficult to compare these color figure together, so the two paths (AB is parallel to the bore with d=2 cm and CD is vertical line) are assumed on the same condition in outside of the both railgun. The graph of the magnetic field intensity (**H**) map on the AB and CD are shown in Fig. 8a and Fig. 8b, respectively. According to the Fig. 8a, the amount of the **H** for slice railgun is larger than rectangular railgun for 0<x<1 cm and less than rectangular railgun for x>1 cm. The distance of the first point of the CD path with edge of the bore is 3 cm. In Fig. 8b, **H** for slice railgun is smaller than rectangular railgun.

3. Multi-Projectile Slice Railgun

By using Slice-Rail railgun, gaining a multi-projectile structure can be achieved easily. If we arrange several Slice-Rail structures beside each other as their inner rails made slices of a cylinder, then we can use a complete cylinder instead of all inner rails.

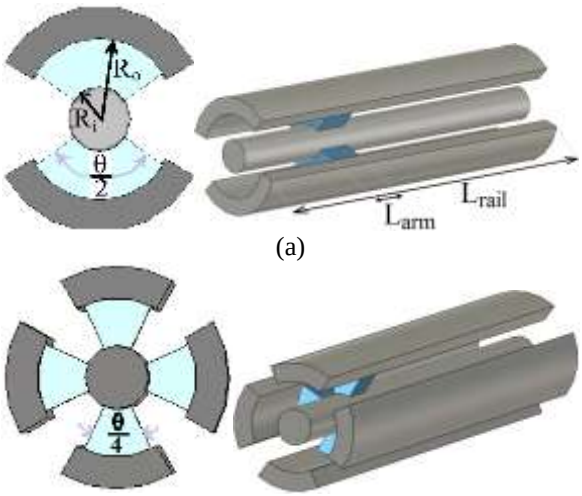

Fig. 9. Cross-Section of Multi-Projectile slice-rail railguns. (a) Dual-Projectile, (b) Quad-Projectile

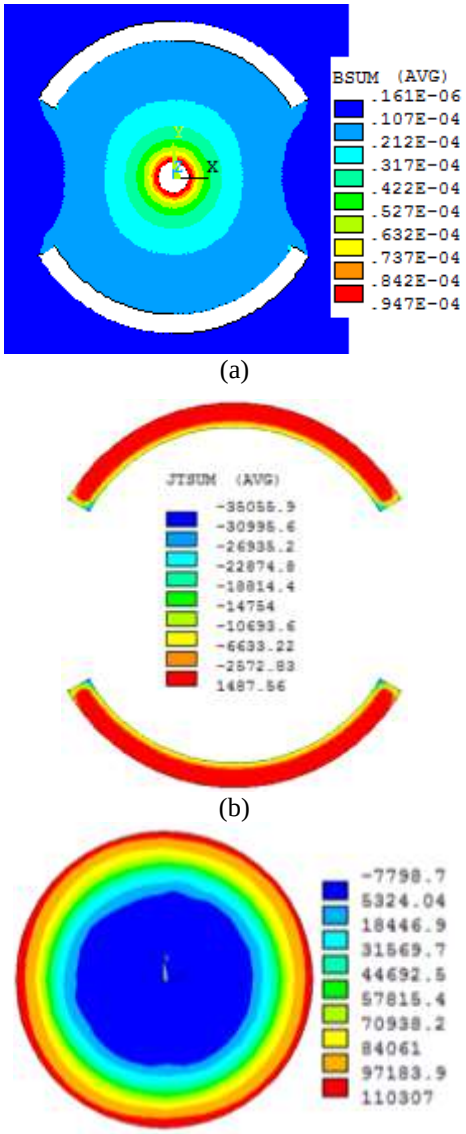

Fig. 10. Slice railgun with dual-projectile and R_i=4 mm, R_o=35 mm and θ_t=240°. (a) magnetic flux density distribution, and the current density distribution on the cross-section of the, (b) outer rails, (c) inner rail.

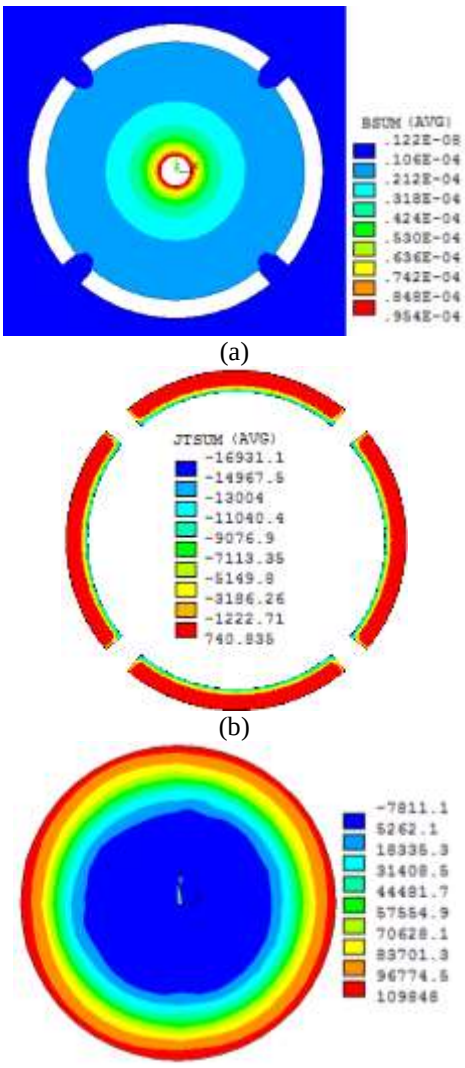

Fig. 11. Slice railgun with quad-projectile and R_i=4 mm, R_o=35 mm and θ_t=320°. (a) magnetic flux density distribution, and the current density distribution on the cross-section of the, (b) outer rails, (c) inner rail.

The geometry of a Dual-Projectile and a Quad-Projectile slice-rail railgun has been shown in Fig. 9 where R_i, R_o and θ are inner rail radii, outer rail radii, and the total angle of curved rails correspondingly, as in single Slice-Rail structure.

It is an easier method to make a Multi-Projectile launcher in comparison of other plain methods. Especially, repulsing forces between rails are not limiter here. In plain methods, holding rails needs more consideration and design of a Multi-Projectile railgun with more armatures are not as easy as here. Here, we have an N-Projectile railgun only with taking θ_i<360°/N. We should use N Slice-Rail structures with lesser θ in order to containment embedding and packing.

The magnetic flux density and current density distribution on rails cross-section for a slice railgun with dual and quad-projectile have been simulated and shown in Figs. 10 and 11, respectively. A slice railgun with dual-projectile has R_i=4 mm, R_o=35 mm and θ_P=120° for each projectile and total θ equals to 240°. A slice railgun with quad-projectile has R_i=4 mm, R_o=35 mm, θ_P=80° for each projectile and total θ equals to 320°.

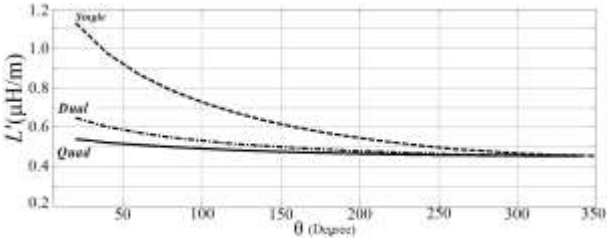

Fig. 12. The gradient inductance L' versus angle θ for single slice-projectile, dual-projectile and quad-projectile.

The gradient inductance L' versus angle θ and R_o/R_i=9 for single slice-projectile, dual-projectile and quad-projectile railguns have been shown in Fig. 12. For all type inductance gradient is descending function as θ. According to Fig. 5. for single slice railgun maximum value of current density for θ smaller than 90˚ is very high and not suitable for practical railgun.

4. Coaxial railgun

A coaxial railgun is a structure with two concentric cylindrical conductors in which the armature, a ring cylindrical conductor completes the path of current between two cylinders as inner and outer rails. The geometry of Coaxial-rail railgun is shown in Fig. 13 where R_i and R_o are inner rail radii and outer rail radii respectively. Likewise slice-rails, R_1 determines the widths of inner rail and R_2 does the same for outer rail. To distinct the effects of rail widths on the structure performance, the inner rail width R_i-R_1 and outer rail width R_2 has been considered as W_i and W_o, respectively.

Because of symmetry, there is no consideration about imposed forces upon rails. The force upon rails is radial and the net value is insignificant. In the view of force distribution on rails and current density distributions the coaxial structure is the best among slice-rail. Fig. 14a, b and c show the magnetic flux density, current density distribution on the outer and inner rails, respectively. According to Fig. 14. b and c, the current distribution is uniform. For Ri=6.35 mm and R_o=37.75 mm L' is obtained to be 0.3696 μH/m, which is slightly different from 0.356 μH/m [17].

The results of simulations have been summarized as follows: Rail width has no significant effects on gradient inductance of the structure and even current density distribution. The only consideration is that the rail width should be enough thick, at least 4 or 5 mm. To determine the effect of rail width on current density distribution in rails we considered the maximum value of current density in each rail. There was an insignificant reduction in the maximum value current density in the thicker rails.

The inductance gradient of coaxial railgun depends on the values of inner radii, R_i and outer radii, R_o. It is obvious that by increasing the value of outer radii, the value of L' increases and vice versa. The behavior of L' versus inner radii is contrariwise, therefore by decreasing the value of inner radii, the value of L' increases and vice versa. Attaining higher values of L' can be manipulated by choosing proper value of the ratio of R_o/R_i. As it has been shown in Fig. 15, the gradient inductance has a direct relation to the R_o/R_i ratio for various inner radii (R_i=4, 6 and 10 mm) and compared with [16].

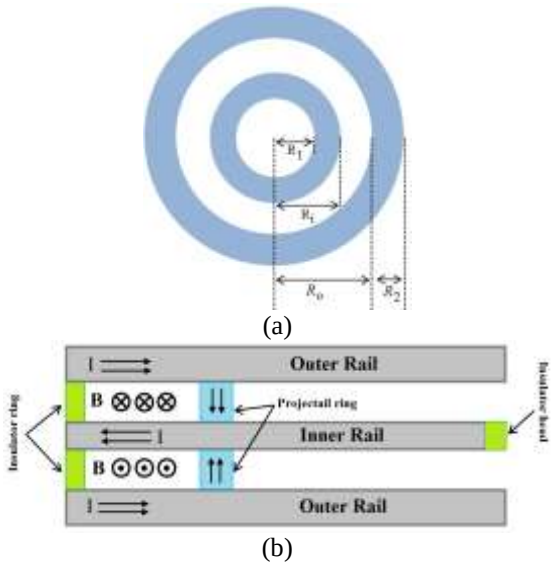

(a)

(b)

Fig. 13. Coaxial railgun. (a) cross section of the rails, (b) practical considerations in coaxial railgun.

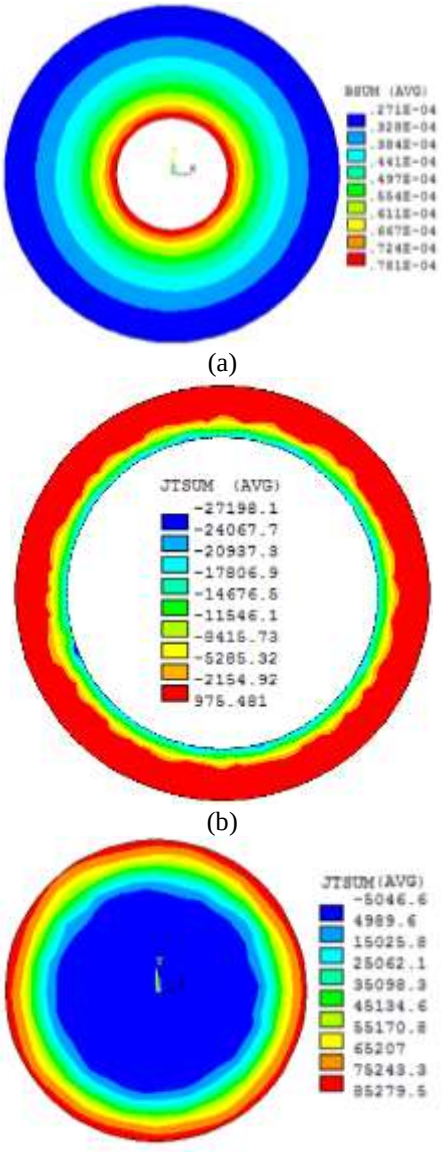

(a)

(b)

(c)

Fig. 14. Coaxial railgun, R_i=5 mm, R_o=15 mm and R_1=20 mm. (a) magnetic flux density distribution, and the current density distribution on the cross-section of the, (b) outer rails, (c) inner rail.

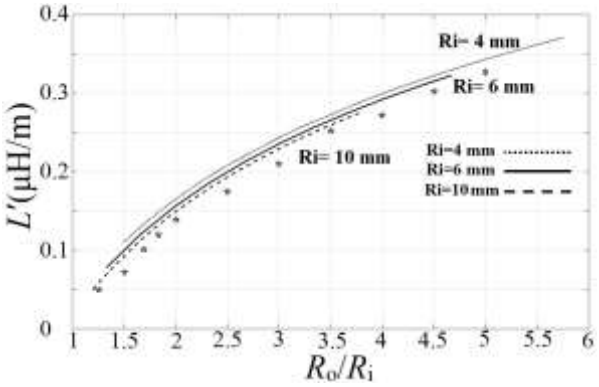

Fig. 15. The Inductance Gradient Versus R_o/R_i ratio, Ri=4 mm (dot), Ri=6 mm (line), Ri=10 mm (dash) and [16] (*).

As we can see in Fig. 15, in a constant value of R_o/R_i the L' has a higher value for a smaller R_i. The ratio of R_o/R_i must be bigger than 4, in order to have L's comparable with parallel railgun's which is more than 0.3 μH/m. Due to skin effect, the L' has minimal dependency on proper value of R_i and R_o.

There are some practical problems with coaxial railgun that maybe seem limiter. First issue is that how we can hold inner rail during launch process and the second is the possibility of inner rail fluctuation when ring armature has been projectile from the muzzle. In order to hold inner rail, especially when railgun length is not very long, we can use a solid insulator ring between rails in the first ten percent of railgun length at the breech.

5. Conclusion

In this paper the slice-rail structure as an unequal-rail parallel railgun and its complete case as coaxial railgun has been studied. The possibility of making Multi-Projectile railgun using pairs of Slice-Rail structures has been approved. The magnetic field at the outside of the bore for slice railgun is smaller than rectangular railgun. The inductance gradient of a slice-rail structure will be decreased if its angle is increased. That is valid for the maximum value of current density in both rail, too. The gradient inductance of a coaxial railgun is in a direct dependency with the outer rail radii.

6. References

[1] O. Bozic, P. Giese, "Aerothermodynamics Aspects of Railgun-Assisted Launches of Projectiles with Sub- and Low-Earth-Orbit Payloads," *IEEE Transactions on Magnetics*, vol. 43, no. 1, pp. 474-479, 2007.

[2] I. R. McNab, "Progress on hypervelocity railgun research for launch to space," *IEEE Transactions on Magnetics*, vol. 45, no. 1, pp. 381–388, 2009.

[3] J. F. Kerrisk, "Current distribution and inductance calculation for railgun conductors," *Los Alamos National Laboratory* Report no. LA-9092-MS, November 1981.

[4] J. F. Kerrisk, "Electrical and Thermal Modelling of Railgun," *IEEE Transactions on Magnetics*, vol. 20, no. 2, pp. 399-402, 1984.

[5] K.-T. Hsieh, "A Lagrangian formulation for mechanically, thermally coupled electromagnetic diffusive processes with moving conductors," *IEEE Transactions on Magnetics*, vol. 31, no. 1, pp. 604–609, 1995.

[6] N. Sengil, "Implementation of Monte Carlo Method on Electromagnetic Launcher Simulator," *IEEE Transactions on Plasma Science*, vol. 45, no. 5, pp. 1156-1160, 2013.

[7] R. Emadifar, S. Tohidi, M. Feyzi, N. Rostami, M. Eldoromi, "Analysis of Magnet Shape Effect on Cogging Torque and EMF Waveform of AFPM Generators Using FEM Methods," *Tabriz Journal of Electrical Engineering*, vol. 47, no. 3, pp. 1147-1159, 2017(in persian).

[8] A. Darabi, A. Behniafar, H. Tahanian, H. Yoosefi, "Finite Element Modelling of an Inversed Design Circumferential Flux Cylindrical Hysteresis Motor in Steady State Condition," *Tabriz Journal of Electrical Engineering*, vol. 47, no. 3, pp. 1001-1012, 2017(in persian).

[9] A. Musolino, "Finite-Element Method/Method of Moments Formulation for the Analysis of Current Distribution in Rail Launchers," *IEEE Transactions on Magnetics*, vol. 41, no. 1, pp. 387-392, Jan 2005.

[10] B. Kim, Kuo-Ta Hsieh, "Effect of Rail/Armature Geometry on Current Density Distribution and inductance gradient," *IEEE Transactions on Magnetics*, vol. 35, no.1, pp. 413-416 January 1999.

[11] A. Keshtkar, "Effect of rail Dimension on Current Distribution and Inductance Gradient," *IEEE Transactions on Magnetics*, vol. 41, no. 1, pp. 383-386, Jan 2005.

[12] M. S. Bayati and A. Keshtkar, "Novel Study of the Rails Geometry in the Electromagnetic Launcher," *IEEE Transactions on Plasma Science*, vol. 43, no. 5, pp. 1652-1656, 2015.

[13] Richard A. Marshall, "Railgun Bore Geometry Round or Square?" *IEEE Transactions on Magnetics*, vol. 35, no.1, pp. 427-431, 1999.

[14] Y. Zhang, J. Ruan, J. Liao, Y. Wang, Y. Zhang and T. Huang, "Salvo Performance Analysis of Triple-Projectile Railgun," *IEEE Transactions on Plasma Science*, vol. 41, no. 5, pp. 1421-1425, 2013.

[15] Y. Zhang, J. Ruan, J. Liao, Y. Wang, Y. Zhang and T. Huang, "Comparison of Salvo Performance Between Stacked and Paralleled Double-Projectile Railguns," *IEEE Transactions on Plasma Science*, vol. 41, no. 5, pp. 1410-1415, 2013.

[16] J. C. Schaaf Jr, N. F. Audeh "Solid Armature Coaxial Railgun Experiment Results," *IEEE Transactions on Magnetics*, vol. 25, no.1, pp. 711-715, 1993.

[17] J. C. Schaaf Jr, N. F. Audeh "Electromagnetic Coaxial Railgun," *IEEE Transactions on Magnetics*, vol. 25, no.5, pp. 3263-3265, 1989.